

Fermi-Liquid-Based Theory for the In-Plane Magnetic Anisotropy in Untwinned High- T_c Superconductors

I. Eremin¹ and D. Manske²

¹*Institut für Theoretische Physik, Freie Universität Berlin, Arnimallee 14, D-14195 Berlin, Germany*

²*Max Planck Institut für Festkörperforschung, Heisenbergstrasse 1, D-70569 Stuttgart, Germany*

(Received 26 July 2004; published 17 February 2005)

Using a generalized RPA-type theory we calculate the in-plane anisotropy of the magnetic excitations in hole-doped high- T_c superconductors. Extending our earlier Fermi-liquid-based studies on the resonance peak by inclusion of orthorhombicity we still find two-dimensional spin excitations, however, being strongly anisotropic. This reflects the underlying anisotropy of the hopping matrix elements and of the resultant superconducting gap function. We compare our calculations with new experimental data on *fully untwinned* YBa₂Cu₃O_{6.85} and find good agreement. Our results are in contrast to earlier interpretations on the in-plane anisotropy in terms of stripes [H. Mook *et al.*, Nature (London) **404**, 729 (2000)], but reveal a conventional solution to this important problem.

DOI: 10.1103/PhysRevLett.94.067006

PACS numbers: 74.25.Ha, 74.20.Mn, 74.72.Bk

Since the discovery of high- T_c superconductors, its mechanism is still under debate. Perhaps one of the most important questions concerns the role played by spin excitations in these materials. For example, one scenario of superconductivity in layered cuprates suggests that Cooper-pairing is due to an exchange of antiferromagnetic spin fluctuations [1]. In this respect, an understanding of the so-called resonance peak observed by inelastic neutron scattering (INS) experiments [2,3] at the antiferromagnetic (AFM) wave vector \mathbf{Q}_{AFM} and energy $\omega \approx \omega_{\text{res}}$ plays an important role in the phenomenology of high- T_c superconductors. Among various explanations over last years there are two most probable scenarios for the formation of the resonance peak. The first one suggests that the two-dimensional CuO₂ layers are intrinsically unstable towards a stripe formation with one-dimensional spin and charge order [4]. In this picture, the resonance excitations can be interpreted in terms of excitation spectra in a bond-centered stripe state with long-range magnetic order [5,6]. In the other approach that is a conventional Fermi-liquid one, the resonance peak arises as a particle-hole excitation (or spin density wave collective mode) in a $d_{x^2-y^2}$ -wave superconductor and is a result of the strong feedback of the superconductivity on the dynamical spin susceptibility below T_c [7–12].

In order to distinguish between both pictures, a detailed analysis of untwinned cuprates is necessary. Recently, an INS study in the fully untwinned high-temperature superconductor YBa₂Cu₃O_{6.85} reveals two-dimensional character of the magnetic fluctuations [13] in contrast to the previous conclusions from measurements in the partially untwinned samples [14]. In this Letter, motivated by recent experiments, we analyze the in-plane anisotropy of the magnetic excitations in hole-doped high- T_c superconductors within a conventional Fermi liquid and generalized RPA-like approach. Extending our earlier studies on the resonance peak by the inclusion of a small orthorhombicity

we still find two-dimensional spin excitations, however being strongly anisotropic, reflecting the underlying anisotropy of the hopping matrix elements and of the resultant superconducting gap function.

In order to describe the phenomenology of the superconducting cuprates we employ an effective one-band Hubbard Hamiltonian for the CuO₂ plane

$$H = \sum_{\langle ij \rangle \sigma} t_{ij} c_{i\sigma}^\dagger c_{j\sigma} + U \sum_i n_{i\uparrow} n_{i\downarrow}, \quad (1)$$

where $c_{i\sigma}^\dagger$ is a creation operator of an electron with spin σ on site i , U denotes the on-site Coulomb repulsion [15], and t_{ij} is a hopping matrix element in the CuO₂ plane. Here, we use the six parameter fit of the energy dispersion suggested in Ref. [17] with the following chemical potential and hopping amplitudes (μ, t_1, \dots, t_5) (the units are in eV): (0.1197, -0.5881, 0.1461, 0.0095, -0.1298, 0.0069). The lattice constants are set to unity. To describe the orthorhombic distortions we introduce a parameter δ_0 which leads to an anisotropy in the hopping integrals along and perpendicular to the chains in YBa₂Cu₃O_{6.85} (YBCO). This one-band approach seems to be justified at least in the optimally-doped cuprates because upon hole doping into the CuO₂ plane antiferromagnetism disappears due to Zhang-Rice singlet formation and quenching of Cu spins. Further doping then increases the carrier mobility and a system of strongly correlated quasiparticles occurs [18].

Normal state.—Before analyzing the superconducting state it is instructive to understand how the normal state properties and the electronic structure of a CuO₂ plane are affected by the presence of the orthorhombic distortions. In Fig. 1 we show the calculated density of states (DOS) and Fermi surface topology as a function of the orthorhombic distortions. Without orthorhombicity the DOS reveals a pronounced van Hove singularity (VHS) being approximately 19 meV below the Fermi level in good agreement with early angle resolved photoemission spectroscopy

(ARPES) experiments on YBCO [19]. Because of the vicinity of the VHS to the Fermi level, the effect of the orthorhombic distortions is quite strong. First, at $\delta_0 = 0.03$ the singularity is suppressed and shifted slightly above the Fermi level. With further increase of δ_0 it splits into two peaks. Similar changes occur for the Fermi surface. As a function of the orthorhombicity its topology changes and the Fermi surface closes around the $(-\pi, 0)$ and $(\pi, 0)$ points which also leaves an impression that the system turns towards a quasi-one-dimensional one. One of the immediate consequence of these changes is that the VHS will be present below the Fermi level only around $(0, \pm\pi)$ points. This is also consistent with more recent ARPES data on untwinned YBCO [20] where a suppression of the ARPES intensity was observed around $(\pm\pi, 0)$ due to absence of the VHS. It is important to note that this Fermi surface deformation breaks the point-group symmetry and looks similar to what is expected for the case of a $d_{x^2-y^2}$ -wave Pomeranchuk instability due to strong electron-electron interactions [21].

What happens to the spin response if the electronic properties are changed due to orthorhombicity? We calculate the real part of the bare spin susceptibility in the normal state,

$$\chi_0(\mathbf{q}, \omega) = \sum_{\mathbf{k}} \frac{f(\varepsilon_{\mathbf{k}}) - f(\varepsilon_{\mathbf{k}+\mathbf{q}})}{\varepsilon_{\mathbf{k}+\mathbf{q}} - \varepsilon_{\mathbf{k}} + \omega + i0^+}, \quad (2)$$

where $f(\varepsilon_{\mathbf{k}})$ is the Fermi function. In Fig. 2 we show the calculated $\text{Re}\chi_0(\mathbf{q}, \omega = 0)$ as a function of the transferred momentum \mathbf{q} . Without orthorhombicity its peak structure reflects two $2\mathbf{k}_F$ instabilities of the Fermi surface (see inset of Fig. 1). The first peak corresponds to the quasi-one-dimensional wave vector connecting the Fermi surface (FS) around $(0, \pm\pi)$ points and the other one refers to the wave vector connecting the FS along the diagonal of the first Brillouin zone. Note that due to strong nesting of the Fermi surface the second structure has the form of a

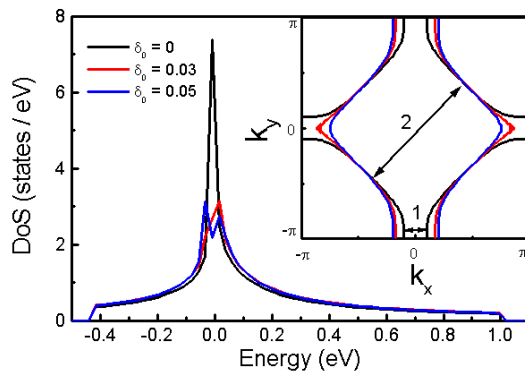


FIG. 1 (color online). Calculated density of states with and without orthorhombicity. For a comparison the corresponding changes of the Fermi surface topology are shown in the inset. The arrows refer to the two $2\mathbf{k}_F$ instabilities as described in the text.

plateau. If the orthorhombicity is present the first peak is suppressed and shifted towards higher \mathbf{q} values. This is due to the fact that the Fermi surface closes around $(\pm\pi, 0)$ point removing this instability there and moving them to higher \mathbf{q} values around $(0, \pm\pi)$ points. On the other hand, the diagonal second $2\mathbf{k}_F$ instability remains mainly unchanged and even became more pronounced, since the plateau around $\mathbf{Q}_{\text{AFM}} = (\pi, \pi)$ is suppressed due to the changes of the Fermi surface topology at the parts connected by this wave vector. We would like to stress that despite the changes of the Fermi surface topology indicating the tendency towards quasi-one-dimensionality, the static spin susceptibility remains mainly two-dimensional.

Superconducting state.—In our one-band model, we further assume that the same quasiparticles are participating in the formation of antiferromagnetic fluctuations and in Cooper-pairing due to these fluctuations. This leads to the generalized Eliashberg equations which have been derived and discussed in Refs. [22,23]. These equations allow us to calculate all properties of the system *self-consistently* such as the elementary excitations, the superconducting order parameter, and the dynamical spin susceptibility, for example.

In the pure tetragonal case the resulting superconducting order parameter has $d_{x^2-y^2}$ -wave symmetry. However, in presence of orthorhombicity the superconducting order parameter changes, since s -wave and d -wave symmetries belong now to the same irreducible representation of the point-group symmetry. The total superconducting gap has the form (weak-coupling limit)

$$\Delta(\mathbf{k}) = g(\delta_0)\Delta_s(\mathbf{k}) + f(\delta_0)\Delta_d(\mathbf{k}), \quad (3)$$

where, for simplicity, we employ $g(\delta_0) = \delta_0$, $f(\delta_0) = 1 - \delta_0$, and $\Delta_d = \Delta_0(\cos k_x - \cos k_y)/2$, $\Delta_s = \Delta_0(\cos k_x + \cos k_y)$. For the set of parameters described above, we use $\Delta_0 = 26$ meV. Note that the additional s -wave component leads to an in-plane anisotropy of the gap function and thus to different maximum gap values between $(\pm\pi, 0)$ and $(0, \pm\pi)$ as observed in Ref. [24].

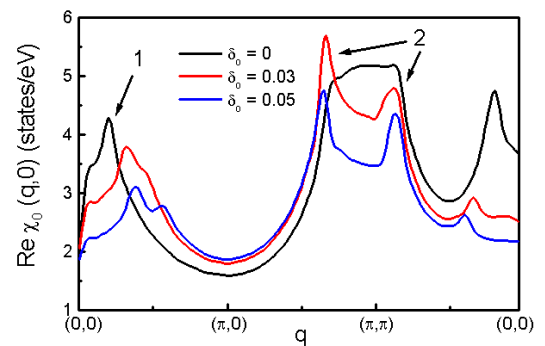


FIG. 2 (color online). Calculated $\text{Re}\chi_0(\mathbf{q}, 0)$ along the path $(0, 0) \rightarrow (\pi, 0) \rightarrow (\pi, \pi) \rightarrow (0, 0)$ for various values of the orthorhombic distortions. The arrows indicate the peaks in $\text{Re}\chi_0(\mathbf{q}, 0)$ arising from $2\mathbf{k}_F$ instabilities as shown in Fig. 1.

In the superconducting state, within generalized RPA, the imaginary part of the dynamical spin susceptibility is given by

$$\text{Im}\chi(\mathbf{q}, \omega) = \frac{\text{Im}\chi_0(\mathbf{q}, \omega)}{[1 - U\text{Re}\chi_0(\mathbf{q}, \omega)]^2 + U^2\text{Im}\chi_0^2(\mathbf{q}, \omega)}, \quad (4)$$

where χ_0 is the BCS Lindhard response function [17]. Without orthorhombicity, the $d_{x^2-y^2}$ superconducting gap opens rapidly due to a feedback effect on the elementary excitations [25] yielding a jump at $2\Delta_0$ in $\text{Im}\chi_0$ and the resonance condition [7–9]

$$1 - U\text{Re}\chi_0(\mathbf{q} = \mathbf{Q}_{\text{AFM}}, \omega = \omega_{\text{res}}) = 0 \quad (5)$$

is fulfilled. Since $\text{Im}\chi_0$ is zero below $2\Delta_0$, the resonance condition (5) reveals a strong deltalike peak in $\text{Im}\chi_0$ which occurs only below T_c . Note that its position is mainly determined by the maximum of the d -wave superconducting gap Δ_0 and also by the proximity to an antiferromagnetic instability described by the characteristic energy scale ω_{sf} [roughly the peak in $\text{Im}\chi(\mathbf{Q}_{\text{AFM}}, \omega)$ in the normal state]. Then, the resonance peak scales with the maximum of the d -wave superconducting gap in optimally-doped and overdoped compounds. On the other hand, in the underdoped cuprates it rather scales with ω_{sf} [7–9] due to stronger antiferromagnetic fluctuations. Thus, one finds for the whole doping range $\omega_{\text{res}}/k_B T_c \approx \text{const}$ [7–9] in good agreement with experiments [26].

In Fig. 3 we analyze the influence of the orthorhombic distortions on the resonance peak. One clearly sees that the orthorhombicity slightly shifts the resonance peak towards higher energies and reduces its intensity for increasing δ_0 . As already mentioned, the position of the resonance peak is determined by the strength of the antiferromagnetic fluctuations

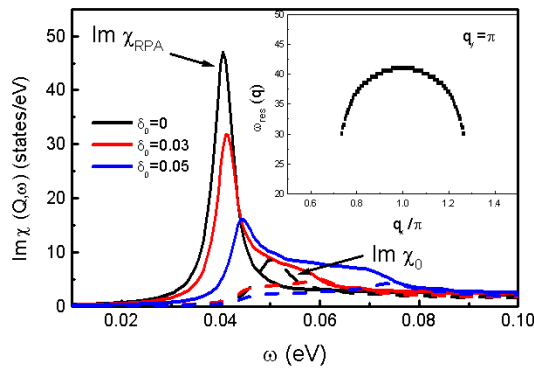


FIG. 3 (color online). Calculated influence of the orthorhombic distortions (s -wave component of the superconducting gap and changes in the electronic structure) on the resonance peak. Inset: calculated dispersion of the resonance peak towards lower energies for fixed $q_y = \pi$ without including the effect of the orthorhombicity. Here, in order to fit the position of the resonance at \mathbf{Q}_{AFM} around 41 meV we use $U = 0.155$ eV. Note that we further employ the damping $\Gamma = 2.4$ meV.

present in the normal state and by the d -wave superconducting gap. Both are decreasing due to orthorhombicity. Namely, as one sees from Fig. 2, the susceptibility is decreasing around \mathbf{Q}_{AFM} due to a change of the Fermi surface topology. Thus, in the superconducting state the resonance is shifted towards higher energies. On the other hand, the maximum of the d -wave gap is decreasing [as we see from Eq. (3)] which would shift the resonance energy towards lower values. Most importantly, we see that the deformation of the electronic structure and FS topology due to orthorhombicity dominate the effect from considering solely the increase of the s -wave component of the superconducting gap. Thus, we conclude that the observed slight shift of the resonance peak position in untwinned YBCO [13] occurs due to the strong changes in the electronic structure induced by the orthorhombic distortion rather than due to additional s -wave component of the superconducting gap.

Comparison with experiment.—Let us now turn to the broader analysis of the dispersion of the resonance excitations below ω_{res} . In the tetragonal case, going away from the points of the Fermi surface connected by the antiferromagnetic wave vector \mathbf{Q}_{AFM} , we are moving towards the diagonal of the BZ where the $d_{x^2-y^2}$ -wave superconducting gap is zero. As a result the resonance energy, ω_{res} shifts towards smaller values. This results in the parabolic shape of resonance energy dispersion as shown in the inset of Fig. 3 calculated for fixed $q_y = \pi$. This parabolic behavior obtained in our calculations agrees well with the experimental findings of Bourges *et al.* [26].

We also would like to stress that the simple parabolic shape of the downward dispersion of the resonance can be further influenced by a strong momentum dependence of the effective interaction U . In principle, if U is decreasing away from (π, π) , it would tend to shift the resonance to the higher energies. Consequently, the downward dispersion will be more a complicated function of $U_{\mathbf{q}}$ and $\Delta_{\mathbf{q}}$. Based on the simple parabolic shape of the resonance peak dispersion which is observed experimentally, we can conclude that at least in optimally and overdoped cuprates the momentum dependence of U is relatively weak. This is probably not the case for the underdoped compounds.

What is happening *below* the resonance threshold ($\omega < \omega_{\text{res}}$) in fully untwinned YBCO for constant energy scans as a function of the momenta q_x and q_y ? In Fig. 4 we show the calculated projected momentum dependence of $\text{Im}\chi(\mathbf{q}, \omega = 35 \text{ meV})$ without (a) and with (b) orthorhombicity. In accordance with *ab initio* calculations, we have chosen $\delta_0 = 0.03$ [27]. In the tetragonal case one sees that the spin excitations form a ring around (π, π) with four pronounced peaks at $(\pi \pm q_0, \pi)$ and $(\pi, \pi \pm q_0)$. The origin of the peaks is clear: away from \mathbf{Q}_{AFM} we are connecting points at the Fermi surface which lie closer to the diagonal of the BZ. The superconducting gap tends to zero there and thus the position and the intensity of the resonance peak are decreasing. However, for the diagonal

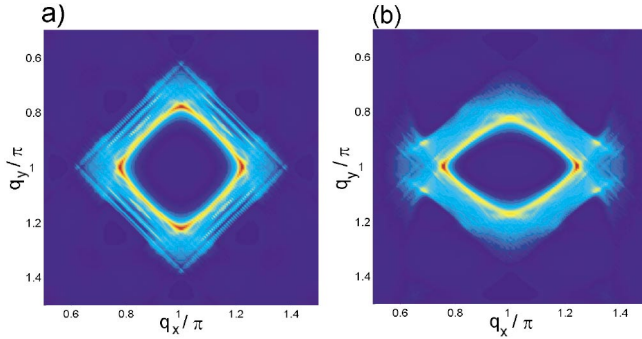


FIG. 4 (color). Calculated normalized two-dimensional intensity plot for a constant energy of $\hbar\omega = 35$ meV, (a) without, (b) with inclusion of orthorhombicity ($\delta_0 = 0.03$).

wave vectors $(\pi \pm q_0, \pi \pm q_0)$ it happens faster than for the vector $(\pi \pm q_0, \pi)$ or $(\pi, \pi \pm q_0)$. Therefore, effectively the latter peaks are “closer” to the resonance condition at $\mathbf{Q}_{\text{AFM}} = (\pi, \pi)$; their intensities are higher than those for the other wave vectors. This explains the observed symmetry of the dominant spin excitations for $\omega < \omega_{\text{res}}$ shown in Fig. 4(a). For the orthorhombic case the situation is changing. The ring of the excitations becomes distorted and, most importantly, there are only two well pronounced peaks. The latter is a result of strongly changed electronic properties, in particular, the topology of the FS. Our *main result* is that, despite there are only two pronounced peaks, the resonant spin excitations remains basically two-dimensional. This is in good agreement with recent experiments [13]. Furthermore, this result based on a standard Fermi-liquid approach is in contrast to the stripe scenario of the resonance peak [5]. Another interesting observation is that the dispersion will have a different slope along q_x and q_y direction, respectively. This can be further tested experimentally.

In summary, we have analyzed the in-plane magnetic anisotropy in high- T_c superconductors with orthorhombic distortions employing a generalized RPA-type theory and compared our results with INS data on fully untwinned YBCO. We find that due to changes in the electronic structure and the FS topology the resonance peak is slightly shifted towards higher energies and that for $\omega < \omega_{\text{res}}$ the dominant spin excitations form a 2D ringlike structure around \mathbf{Q}_{AFM} with four pronounced peaks (tetragonal case). The orthorhombic distortions suppress two of these peaks; however, the overall structure of the excitations in $\text{Im}\chi$ remains two-dimensional which agrees well with recent experimental data by V. Hinkov *et al.* [13]. Our results provide an alternative picture based on a conventional Fermi-liquid theory in contrast to the stripe scenario.

It is a great pleasure to acknowledge our cooperation with V. Hinkov, B. Keimer, and Ph. Bourges and thank them for enlightening discussions and providing us their data prior to publication. We also wish to thank A. Chubukov, D. K. Morr, S. Pailhes, Y. Sidis, D. Reznik, and K. H. Bennemann for valuable discussions. Financial

support by INTAS (No. 01-0654) is gratefully acknowledged.

-
- [1] See, for review, D. Scalapino, Phys. Rep. **250**, 327 (1995); Ar. Abanov, A. V. Chubukov, and J. Schmalian, Adv. Phys. **52**, 119 (2003).
 - [2] H. F. Fong *et al.*, Phys. Rev. B **61**, 14773 (2000).
 - [3] Ph. Bourges, L. P. Regnault, Y. Sidis, and C. Vettier, Phys. Rev. B **53**, 876 (1996).
 - [4] See, for review, S. A. Kivelson, Rev. Mod. Phys. **75**, 1201 (2003).
 - [5] M. Vojta and T. Ulbricht, Phys. Rev. Lett. **93**, 127002 (2004); G. S. Uhrig, K. P. Schmidt, and M. Grüninger, *ibid.* **93**, 267003 (2004).
 - [6] G. Seibold and J. Lorenzana, cond-mat/0406589.
 - [7] D. Manske, I. Eremin, and K. H. Bennemann, Phys. Rev. B **63**, 054517 (2001).
 - [8] F. Onufrieva and P. Pfeuty, Phys. Rev. B **65**, 054515 (2002).
 - [9] A. Abanov, A. V. Chubukov, M. Eschrig, M. R. Norman, and J. Schmalian, Phys. Rev. Lett. **89**, 177002 (2002).
 - [10] D. K. Morr and D. Pines, Phys. Rev. Lett. **81**, 1086 (1998).
 - [11] I. Sega, P. Prelovsek, and J. Bonca, Phys. Rev. B **68**, 054524 (2003).
 - [12] J.-X. Li and C.-D. Gong, Phys. Rev. B **66**, 014506 (2002); T. Zhou and J.-X. Li, Phys. Rev. B **69**, 224514 (2004).
 - [13] V. Hinkov, S. Pailhes, P. Bourges, Y. Sidis, A. Kulakov, C. T. Lin, C. Bernhard, and B. Keimer, Nature (London) **430**, 650 (2004).
 - [14] H. A. Mook, P. Dai, F. Dogan, and R. D. Hunt, Nature (London) **404**, 729 (2000).
 - [15] Note that generally the effective interaction U can be strongly momentum dependent and peaked at the antiferromagnetic wave vector $\mathbf{Q}_{\text{AFM}} = (\pi, \pi)$ as was shown previously [16].
 - [16] Q. Si, J.-P. Lu, and K. Levin, Phys. Rev. B **45**, 4930 (1992).
 - [17] M. R. Norman, Phys. Rev. B **63**, 092509 (2001); O. Tchernyshyov, M. R. Norman, and A. V. Chubukov, Phys. Rev. B **63**, 144507 (2001).
 - [18] In this one-band picture the Coulomb interaction U between these quasiparticles refers to an effective interaction within the conduction band and thus is smaller than the bandwidth.
 - [19] K. Gofron *et al.*, Phys. Rev. Lett. **73**, 3302 (1994).
 - [20] M. C. Schabel *et al.*, Phys. Rev. B **57**, 6090 (1998); **57**, 6107 (1998).
 - [21] W. Metzner, D. Rohe, and S. Andergassen, Phys. Rev. Lett. **91**, 066402 (2003).
 - [22] D. Manske, *Theory of Unconventional Superconductors* (Springer, Heidelberg, 2004).
 - [23] D. Manske, I. Eremin, and K. H. Bennemann, Phys. Rev. B **67**, 134520 (2003).
 - [24] D. H. Lu *et al.*, Phys. Rev. Lett. **86**, 4370 (2001).
 - [25] D. Manske, I. Eremin, and K. H. Bennemann, Phys. Rev. Lett. **87**, 177005 (2001).
 - [26] P. Bourges, Y. Sidis, H. F. Fong, L. P. Regnault, J. Bossy, A. Ivanov, and B. Keimer, Science **288**, 1234 (2000).
 - [27] O. K. Andersen, A. I. Liechtenstein, O. Jepsen, and F. Paulsen, J. Phys. Chem. Solids **56**, 1573 (1995).